A Hybrid Defect Detection Method for Wafer level Chip Scale Package Images

[1]Chia-Feng Chang, [2]Jiunn-Lin Wu and [3]Yu-Chun Wang

Abstract

In the majority of semiconductor manufacturing, the visual inspection process of the wafer surface depends on human experts. However, the inefficiencies of human visual inspection has led to the development of image process to perform inspection tasks. The occurrence of different type of defect arises from the manufacturing processed variations, like miss-out calibration or poor maintenance of the equipment. There are several semiconductor inspection approaches have been proposed but the performance is limited by the variations of defect which has different surface shape, texture, intensity, size, etc. Automated inspection methods that have been developed are tuned for the specific object and background in image processing methods. In our case, the problem of defect detection is even more complex. There are different kinds of texture such like, complex surface, variation defect and bright spots which are metal reflect light, the weak spots which are caused by dust and low intensity defect, in our test image.

In this paper, we propose a hybrid inspection approach to detect defect in chip. For high intensity defect, a simple threshold method is firstly used to detect candidate defect which contains defect, bright spots, weak bright spots and noise by the characterization of high intensity. The morphology operations are then used to filter out small candidate defect which is noise. Finally, the support vector machine is used to classified high intensity defect. For low intensity defect, a boundary defect detection algorithm is presented to detect low intensity defect. Experimental results demonstrate the effectiveness and efficiency of the proposed method.

Keywords: Defect detection, Support Vector Machine, Morphology, Hough Transform, Feature Extraction

*Corresponding Author: Jiunn-Lin Wu
(E-mail:jlwu@cs.nchu.edu.tw).
[1]Department of Computer Science and Engineering, National Chung Hsing University, Taichung, Taiwan

1. Introduction

With the increasing the requirement of chip, the semiconductor manufacturing is in the limelight. The process of defect detection is an important issue to assure the chip is defect-free. In recent, the majority of chip surface inspection depends on manual review, and a defect is identified by the human visual judgment. However, there are some limitations of human inspection:

1). Human inspection is slow and is lack of performance.

2). The inspection process can incur significant personnel costs.

3). Human inspection does not ensure high quality because of the inspection error by human fatigue.

4). Due to high production rate, human inspection is not feasible.

Owing to these reasons, using computer vision to perform inspection tasks becomes important issue.For human inspection, it is easy judgment that whether there exists defect or not. But for image process, it is challenging to detect defect accurately due to there are different types of defect is arise which because of the manufacturing process variations, like miss-out calibration or poor maintenance of the equipment. In addition, the position of defect is random and there exists bright spots which are metal reflect light that are easily confuse with defect. As above reasons, there is no method can effectively detect various types of defect. Therefore, automated inspection methods are tuned for the specific object and background in image.

Recently, several inspection methods have been proposed. These methods can be divided into intensity-based approach, gradient-based approach, frequency-based approach, learning-based approach, and hybrid approach. In general, the pixel value changes seriously when defect occurs. Therefore intensity-based inspection approach [1] was presented. The main idea is the defects usually accompany high intensity. Thus a simple thresholding can be applied to defect detection. But it is easy failed when the quality of image is low or the contrast is low. Another inspection approach, called gradient-based approach [2], was proposed. Defect usually led to high contrast. Therefore test image can be transformed into gradient image. The defect with high contrast can be easier detected. But it will fail when the detailed of image has similar contrast.

Above approaches will fail while the intensity of defect or contrast of defect is similar with detailed of background. To solve this problem, frequency-based inspection approach [3] was proposed. Generally, the shape of components on chip is regular. On the contrary, the shape of defect is irregular. Therefore, the test image can be transform from spatial domain into frequency domain. Such methods analyzes frequency image and find the defect. But if the shape of defect is similar with the detail of background, frequency-based inspection approach will fail. Neural network, SVM such learning-based methods [4] are good at complex decision problem. The characteristic of learning-based method is that learning good decision rule from training data instead of tuning parameter for better performance. As a result, many researchers proposed learning-based inspection method recently. But it cost much time at training phase. Furthermore the surface of chip becomes more complex. Using one of above method to detect defect is not enough. Hybrid inspection method [5] was proposed. The main idea is that using specific method to detect specific defect.

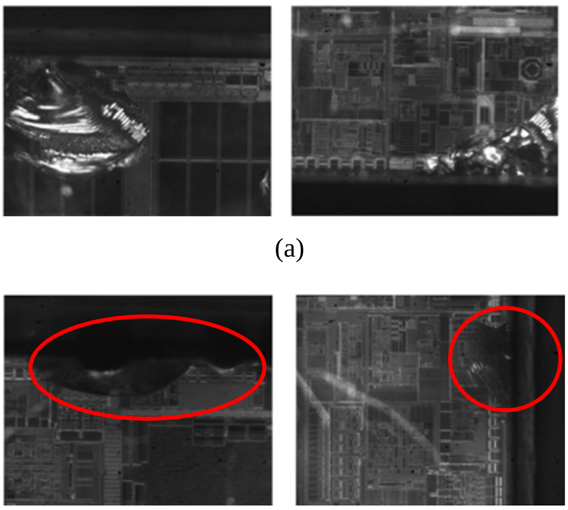

(a)

(b)

Figure 1 Examples of defect on chip. (a) High intensity defect; (b) Low intensity defect.

In this paper, we proposed a hybrid inspection method for wafer level chip. The defects are shown in Figure 1. To observe Figure 1, the type of defect can be divided into high intensity defect and low intensity defect. Therefore we develop different methods for each type of defect. For high intensity defect, a simple threshold method is applied to separate high intensity region, called candidate defect, from background. Because the high intensity region contains not only defects but also light spots and noise. To further extracting defects from candidate defects, it needs more steps. First to remove noise and fill up the contour of candidate, the morphological operation [6] is used. After filling up the contour of defect several features, smoothness, complexity of texture and structure of defect, are computed from each candidate defect. Then above three features are used as inputs for support vector machine (SVM) classifier to judge whether the candidate defect is high intensity defect or not. For correctness of extracted features, we need to correct the rotation of test image. Then for low intensity defect, we proposed a boundary defect detection method. The low intensity defects always appear at the boundary of chip. To find the chip of boundary is the main task for detecting low intensity defect. First we use the information of image intensity to get a coarse contour of chip and then the morphological operations are applied to fill up the contour. Finally, canny edge [7] and Hough transform [8] are used to find the expected boundary, then using the distance between expected boundary and contour of chip to judge whether there exists low intensity defect or not.

2. Related Works

In recent, more and more researches applied learning-based approach to perform defect detection. Comparing with other type of approaches, learning-based approaches need not set any preset parameter but still can solve complex decision problems. Chang et al. (2009) [4] proposed a learning-based approach using neural network classifier for defect detection at various regions on LED die. They adopted radial basis function neural network (RBFNN) as the mapping algorithm, because the RBFNN has advantage of short learning time and good generalization ability in performing the interpolation in the output space. The network learns from the training pairs, which consisting of an input and a desired output, and adjusts weights to minimize the error between the actual and the desired responses. A LED die consists of two main components: the light-emitting area and the p-electrode. Figure 2 shows an example of LED die.

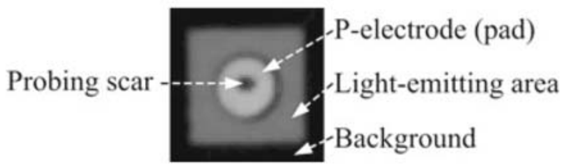

Figure 2 An example of LED die. [4]

For light-emitting area inspection, this area divided into four blocks and the shape of each block is similar to "L". For p-electrode area inspection, the shape of this portion is similar to "O". Thus, in feature extraction step, statistical features and geometric features are measured and then used as inputs for RBFNN. In p-electrode region, the number of pixel in p-electrode region, the mean, standard deviation and one of the deviations that is smaller than standard deviation are extracted as features. And in light-emitting region, this region divided into four blocks can be more easily found because in defective chip, the features change significantly within a small region. The four blocks (L_i) are defined as

$$
\begin{aligned}
L_i &= s_i(x,y) \Big| 0+\frac{m}{k}\operatorname{mod}_k(i) \\
&\le x < \frac{m}{k}[\operatorname{mod}_k(i), 0+\frac{n}{l}\left\lfloor \frac{i}{k} \right\rfloor] \\
&\le y < \frac{n}{l}\left[\frac{i}{k}+1\right], i = 0,1,\ldots,kl-1
\end{aligned} \tag{1}
$$

Where x and y are ranges in the light-emitting area; m and n are the width and height of image, and k = l = 2. Then the features of the mean (*m*), mean square (*ms*), standard deviation (*sd*), mean deviation (*md*) and entropy (*e*), are extracted at each block and are obtained using following equations:

$$F_m^L = \sum_{\forall(x,y)\in L_i}^{s_i(x,y)} / N_{L_i} \tag{2}$$

$$F_{ms}^L = \sum_{\forall(x,y)\in L_i}^{(s_i(x,y))^2} / N_{L_i} \tag{3}$$

$$F_{sd}^L = \sqrt{\sum_{\forall(x,y)\in L} \left|(s_i(x,y) - F_m^L)^2 / N_{L_i}\right.} \tag{4}$$

$$F_{md}^L = \sum_{\forall(x,y)\in L_i}^{s_i(x,y)} \left|s_i(x,y) - F_m^L\right| / N_{L_i} \tag{5}$$

$$F_e^L = -\sum_{\forall(x,y)\in L_i}^{s_i(x,y)} s_i(x,y)\log_2(s_i(x,y)+1) \tag{6}$$

Where $S_i(x,y)$ is an intensity value of L_i at position (x,y). And the feature vector F^L is organized as $(F_m^L, F_{ms}^L F_{sd}^L, F_{md}^L, F_e^L)^T$.

But with the development of semiconductor manufacturing, the surface of chip becomes more complicated. Single approach is inadequate for full inspection. To increase the performance of defect detection, Chen et al. (2013) [5] proposed a hybrid approach to detect the defect on two categories: the circuit and the bump. An example of chip is showed in Figure 3.

For circuit, a test image was compared with the reference image to locate defect. The difference operation is usually used. But considering the image misalignment, they improved the difference operation with a search procedure to modify image difference operation. The difference d_m can be defined as

$$d_m(x,y) = \min\left(\left|R(x+i, y+j) - s(x,y)\right|\right), \tag{7}$$
$$i, j \in [-w/2, w/2]$$

Where $R(x, y)$ and $S(x, y)$ were the gray level at pixel (x, y) in the reference and inspected images; the w defines the size of search window.

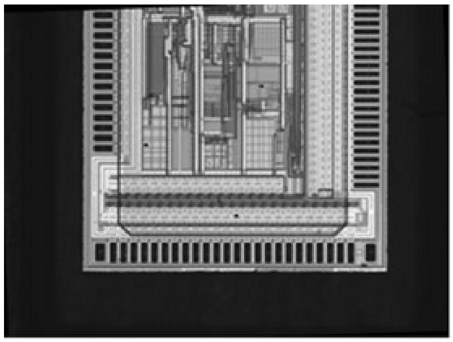

Figure 3 The chip with complicated surface. [5]

When the difference was exceed the specific threshold then the pixel is classified as defective point. For bump, the change of intensity is so tiny that the difference operation is not feasible. The defect of bump was illustrated in Figure 4.

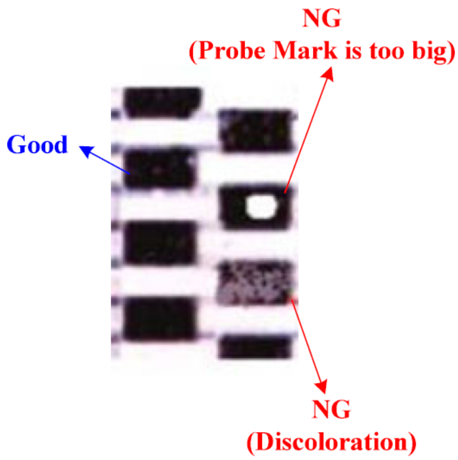

Figure 4 Illustration the defect of bump [5].

The probe mark of defective bump is large than non-defective bump. Therefore, the area and perimeter on the bump are used to judge whether there exists defect on the image.

According to above studies, the hybrid approaches is the efficient method for defect detection. But none of existing methods can efficient detects all type of defect. To effectively perform inspection task using computer vision on the wafer level chip scale package image is our main task. Thus we analyze the characteristics of defect and propose our approach in next section.

3. Proposed Method

In this section, we proposed a hybrid inspection approach for wafer level chip scale package image. As shown in Figure 5, the defects on the chip image was irregular and the detail of background is complicated. Therefore we divide the defects into high intensity defect and low intensity defect, and deal them with different approaches. The flowchart of our proposed inspection method is shown in Figure 6.

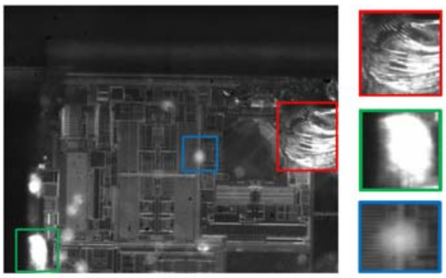

Figure 5 The high intensity regions in the image contain defect and reflections.

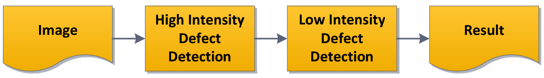

Figure 6 The flowchart of proposed inspection method.

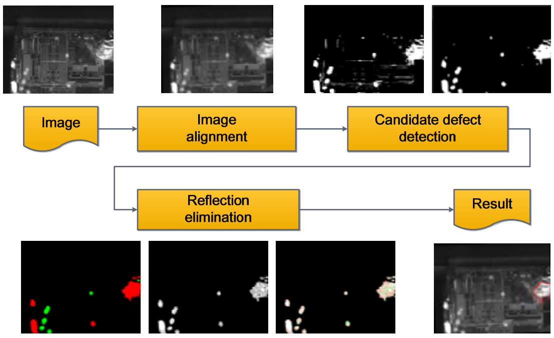

Figure 7 The flowchart of proposed high intensity defect detection.

The goal of the proposed inspection method is to find any defect in the inspected image. Therefore we sequential perform high intensity defect detection and low intensity defect detection. If there exists any high or low intensity defect in the inspected image, then the inspected image is defect image.

For high intensity defect, Hough transform is applied to correct the rotation of test image for precisely measuring information of defect. Then a simple threshold method is applied to separate the high intensity region from background. The high intensity region contains not only defect but also light spot and noise, thus high intensity regions are also called candidate defect. To remove noise and fill up the contour of candidate defect, morphological operations are applied to deal with these tasks. smoothness, complexity of texture and structure of defect are extracted from candidate defect as features for SVM classifier, then a true high intensity defect can be detected. For low intensity defect, as mentioned before, it always appears at boundary of chip. Therefore we can use this characteristic to develop boundary defect detection method. First using threshold method and morphological operations to obtained a satisfied contour of chip. And then Hough transform is used to find the expected boundary. Finally the distance between contour of chip and expected boundary is used to judge whether there exists low intensity defect or not.

Hough transform was well-known method which is used to find the longest line. In our case the boundary of chip has longest line in test image. Therefore Hough transform is used to find the longest line and measure the rotation angle of longest line. The longest line is defined as

$$x\cos\theta + y\sin\theta = \rho \tag{8}$$

where ρ is the perpendicular distance of the line from the origin and θ is the rotation angle from the horizontal of the perpendicular line. According to rotation angle θ, the test image can be rotation to correct position [9]. The correct position (x', y') of original position (x, y) can be computed by

$$\begin{aligned} x' &= x\cos\theta + y\sin\theta \\ y' &= y\cos\theta - x\sin\theta \end{aligned} \tag{9}$$

The result of image alignment is shown in Figure 8. Compare red lines in Figure 8(b) (d), the rotation angle certainly rotates to correct angle.

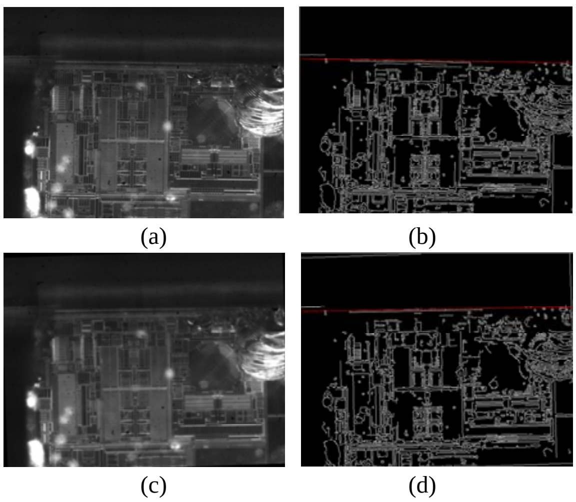

Figure 8 The rotation correction result. (a) Input

image; (b) The detected boundary of chip; (c) After correcting rotation; (d) Corresponding boundary of (c).

After image alignment, we can obtain an input image with correct rotation angle. Then a simple threshold can be applied to separate high intensity region, called candidate defect, from background. The main idea of this step is that to get the higher region on the chip, because the defects always accompany high intensity value. The threshold T is set as

$$T = m_c + \frac{1}{2}\sqrt{\frac{1}{N_c}\sum_{I(x,y)>m_I}(I(x,y)-m_c)} \qquad (10)$$

where mean m_c of the chip area in input image is

$$m_c = \frac{\sum_{I(x,y)>m_I} I(x,y)}{N_c} \qquad (11)$$

Candidate defects contain defect, noise region which is thin and small detail and light spot. Figure 9 shows the result of this step.

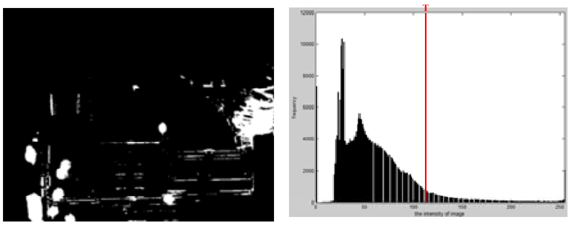

(a) (b)

Figure 9 The result of candidate detection. (a) Candidate defect. (b) Corresponding histogram of (a); the red line indicates the proposed threshold value.

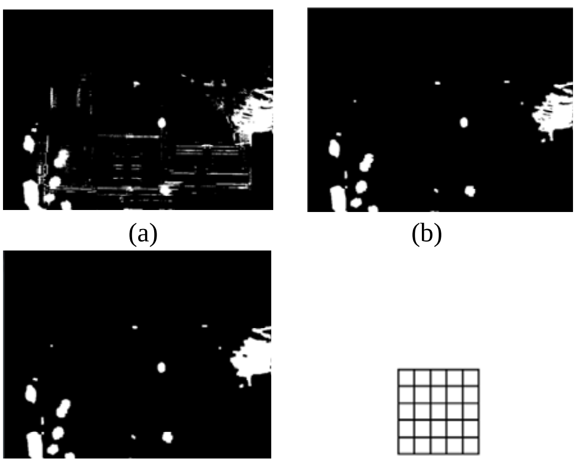

(a) (b) (c) (d)

Figure 10 The effect of small region elimination, (a)Binary image; (b)The result after opening operation; (c) The result after closing operation; (d)The size of structure element is 7x7.

To further filter out noise and fill up the candidate defects, the morphological operations, opening and closing, are applied to deal with them. Figure 10(b) shows that most noise regions had been removed. The rest candidate defects will be defect or light spot. We need further investigate the characteristics of defect and light spot for classifying this candidate defects justness. Observe from Figure 5, the candidate defect can be divided into three types of object which are shown in Figure 11, bright spot, defect and weak spot. Defect and bright spot has higher intensity values than weak spot. And the variance inside bright spot and weak spot are smoother than defect. The structure of weak spot is simpler with vertical and horizontal texture, but the structure of defect is more complex.

(a) (b) (c)

Figure 11 Examples of candidate defects. (a) Bright spot. (b) Defect. (c) Weak-bright spot.

Therefore smoothness, complexity of texture and structure of defect are used as features for learning-based method. The smoothness of candidate defect indicates that change magnitude of pixel values. Therefore standard deviation can be used as the smoothness. The smoothness of candidate defect C_i is defined as

$$\sigma_i = \sqrt{\frac{1}{N_i}\sum\left(I(x,y)-m_I\right)^2} \qquad (12)$$

where m_I is the mean of C_i, $I(x,y)$ is the intensity of pixel in C_i, C_i is ith candidate defect and N_i is the number of pixel in C_i. we set the threshold is 25 and if the smoothness exceeds the threshold than the candidate defect may be real defect or the candidate defect is a light spot. The result of measurement is shown in Figure 12.

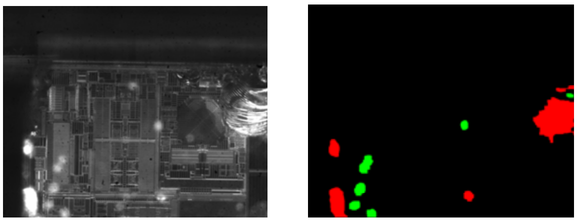

(a) (b)

Figure 12 An example of smoothness of defect. (a) Input image. (b) Result of smoothness measurement; red region indicates the candidate defect may be a real defect, and green region indicates the candidate defect is light spot.

The second feature is complexity of texture. The surface of defect is always complex. So complexity of texture can be simple defined as

$$R_{e_i} = \frac{N_{ei}}{N_i} \tag{13}$$

where N_{ei} is the number of edge in M_i, and M_i is the corresponding canny edge map [7] of C_i. The result of complexity of texture is shown in Figure 13. There are more edges exists in region of defect. On the contrary, there are less edges exists in light spot. The final feature is the structure of defect.

The structure of defect is always complex, we can observe from figure 14. And the structure of a weak spot light is more simple. Because the weak spot does not hide the detail of background, the structure of weak spot is similar with background. Therefore a simple spatial filter can be applied to verify the structure. If there exists any pixels in diagonal direction of target pixel, this pixel is not the detail of background. As shown in Figure 15, the proposed spatial filter can be formulated as

$$R(x,y) = \sum_{a=-1}^{1}\sum_{b=-1}^{1} w(s,t)f(x+s, y+t) \tag{14}$$

If the response of R is not 0, the pixel at (x,y) is detective pixel. Else the pixel at (x,y) is the detail of background. To avoid larger number of edge dominate the result of detection, we use a skew ratio between red pixel and green pixel in candidate defect as the final feature. The skew ratio r_i is defined as

$$r_i = \frac{N_{r_i}}{N_{g_i} + N_{r_i}} \tag{15}$$

where r_i is the skew ratio in C_i, N_{gi} is the number of pixel which is not skew in C_i, and N_{ri} is the number of pixel which is skew in C_i. We use canny edge map as input for the proposed spatial filter, and the result is shown in Figure 16. In Figure 16, the green color indicate target pixel belongs to detail of background and the red color indicates the target pixel belongs to defective pixel. And the result shows that the region inside the defect has more red pixel, and the region of light spot is not. Finally, we use the well-known SVM classifier [10] to judge which is defect according to above three features.

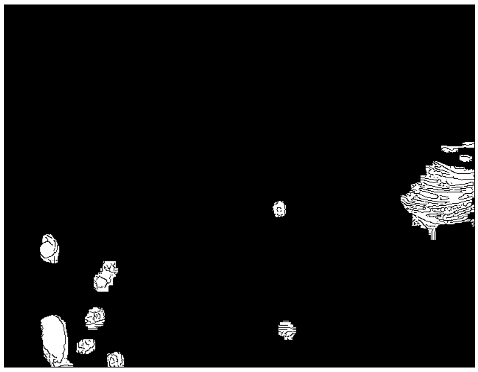

Figure 13 The result of canny edge.

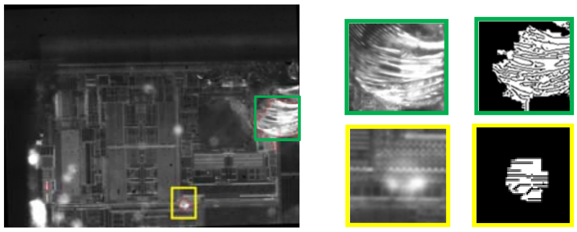

(a) (b) (c)

Figure 14 Examples of complexity of texture. (a) Input image；(b) The upper row is defect and bottom row is weak spot. (c) Corresponding canny edge map of (b).

w(-1,-1)	*w(-1,0)*	*w(-1,1)*
w(0,-1)	*w(0,0)*	*w(0,1)*
w(1,-1)	*w(1,0)*	*w(1,1)*

(a)

1	0	1
0	0	0
1	0	1

(b)

Figure 15 Proposed spatial filter (3x3). (a) The mask *w*. (b) The proposed spatial filter.

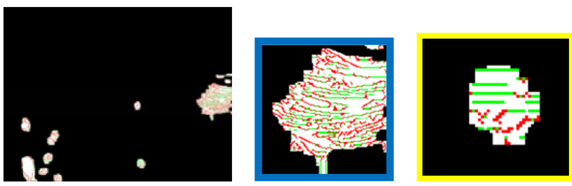

(a) (b) (c)

Figure 16 Examples of structure of candidate defect. (a) The result of structure measurement. (b)

The structure of defect. (c) The structure of light spot.

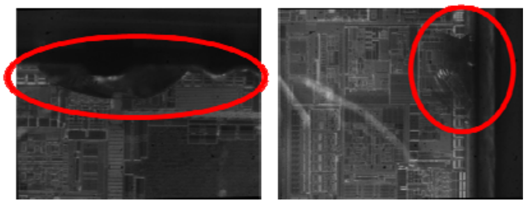

Figure 17 Examples of low intensity defect

Observing the low intensity defect in Figure 17, the defects always appear at the boundary of chip. Extracting accurate contour of chip will be a great help for detecting low intensity defect. Then we proposed a boundary defect detection to solve it. The flowchart of proposed boundary defect detection algorithm is shown in Figure 18.

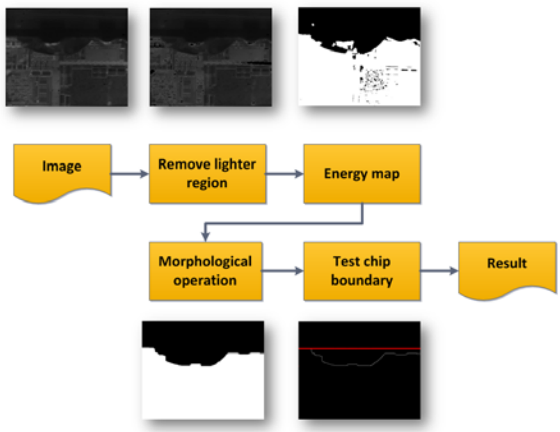

Figure 18 The flowchart of proposed low intensity defect detection algorithm.

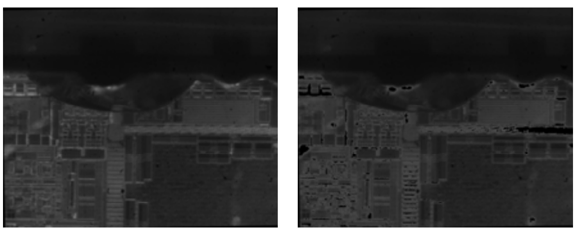

(a) (b)

Figure 19 Examples of remove lighter region. (a) Original Image; (b) After removing lighter region called remaining image.

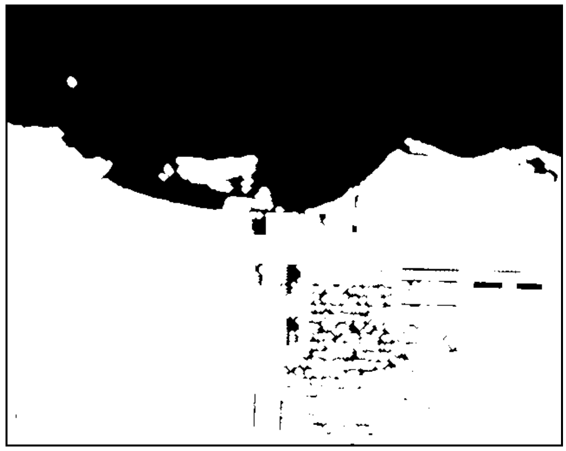

Figure 20 Energy Map.

A simple threshold method using mean of input image can separate the chip from background. But the high intensity regions are too light that raise the mean of image, it will lead to fail in separate chip from background. So the lighter regions are not considered while computing the mean of image. Figure 19 shows the unconsidered lighter regions. Then the mean is used for threshold method. But if we only consider the target pixel as the threshold judgment, the contour of chip will be uneven and hard to find the boundary. Thus we consider all pixels around the target pixel in a window to be the threshold judgment. The formulation is defined as

$$E(x,y) = \begin{cases} 255 & \exists i > m_I, i \in W \\ 0 & \text{else} \end{cases} \tag{16}$$

Where m_I is the mean of remaining image, W is the local window. Then an energy map E can be obtained, the map is shown in Figure 20.

To remove noise and undesired region, we pick the contour with largest contour which is shown in Figure 21. To smooth the boundary and fill up contour the morphological operations, closing and opening, are applied to deal with these tasks. The result of morphological operations is shown in Figure 22. Then the canny edge is applied to get the contour with thinning edge. Finally, we use Hough transform to find the expected boundary, and measure the distance between expected boundary and contour of chip. If number of pixel in contour which is far from expected boundary is too much, then the input image has low intensity defect. The contour of chip and the expected boundary are show in Figure 23 and Figure 24 respectively.

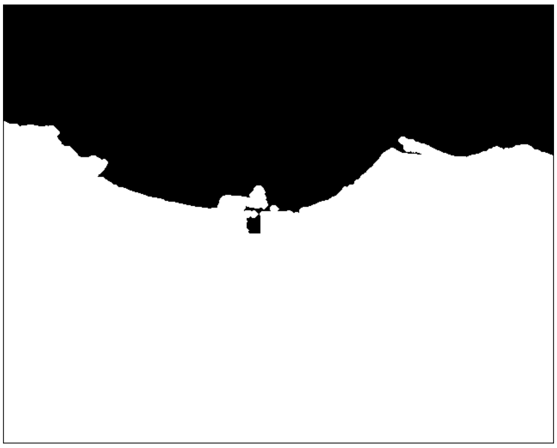

Figure 21 The contour with largest area.

Figure 22 After filling up the contour by morphological operation.

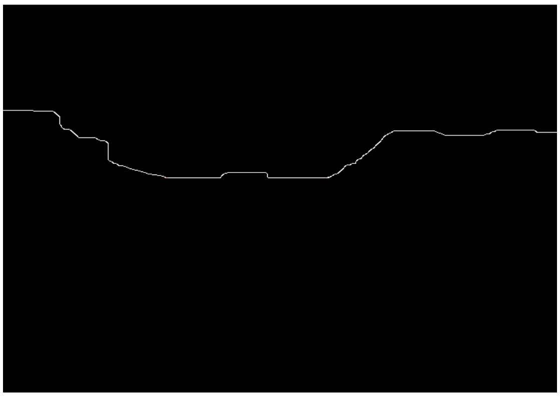

Figure 23 The contour of chip.

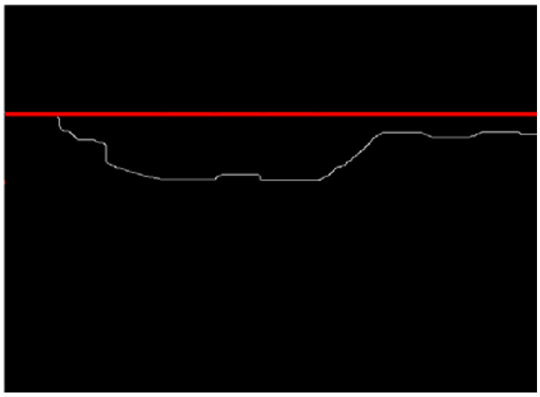

Figure 24 Expected boundary of chip and contour of chip. The red line is expected boundary, and the while line is the contour of chip.

4. Experiment and Discussion

In this section, we use three experiments for verify our proposed method. The first experiment is designed to verify proposed high intensity defect detection algorithm. We use several test images which contain many defects with different size and shape and some of test images also contain light spots to verify the robustness and accuracy of our proposed method. The second experiment is to verify proposed low intensity defect detection. The low intensity defect is very different from the high intensity defect. And the final experiment, we will verify the proposed inspection method. We use 137 inspected images for our experiments. The 137 inspected images include 53 high intensity images, 16 low intensity images and 68 defect-free images. We classify these inspected images using human vision.

In the first experiment, we use 14 inspected images as training data and use all 137 inspected images as test images for our experiment. The detection result is shown in Figure 25. The region which is encircled by red line is detected defect. The result shows that most of defects are detected and the position of defects can be also located. Figure 26 and Figure 27 show that all intermediate results of high intensity defect detection. Among these features, the structure of defect clearly indicates that the defect contains more slope line and the non-defect region contains less slope line. We can see that the proposed features, smoothness, complexity of texture and the structure of defect, can detect the defect efficiently.

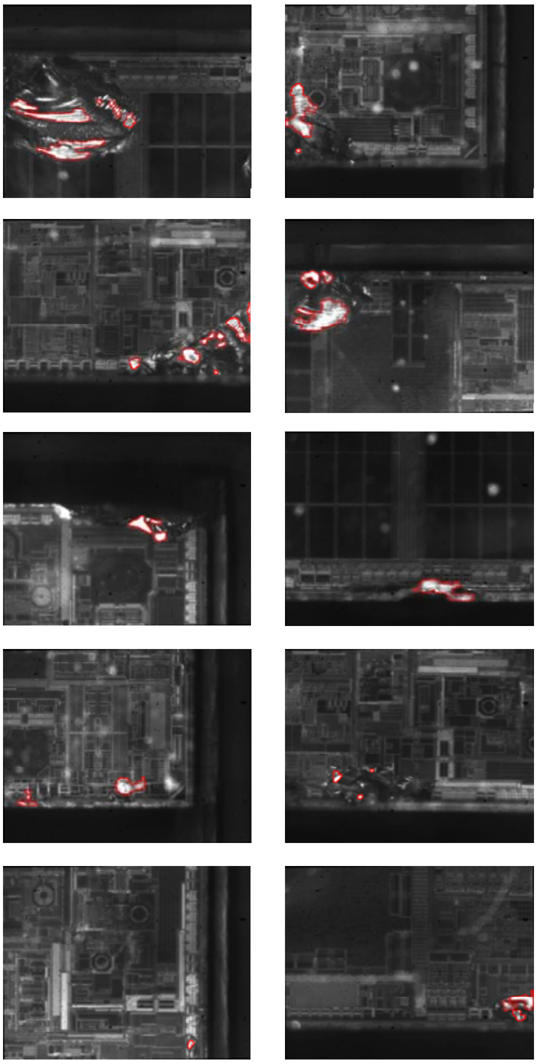

Figure 25 The result of our proposed method. The regions which are encircled by red line are detected defect.

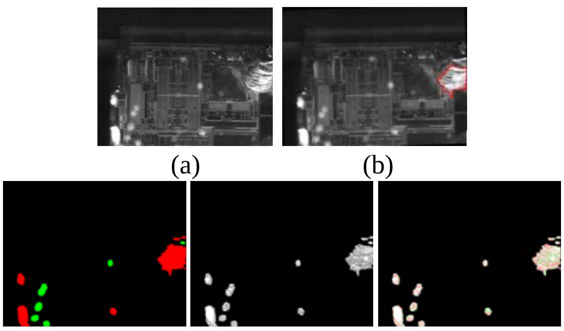

(a) (b)

(c) (d) (e)

Figure 26 The result of reflection elimination using image I as input. (a) The final result. (b) The smoothness of candidate defect. (c) The complexity of texture. (d) The structure of defect.

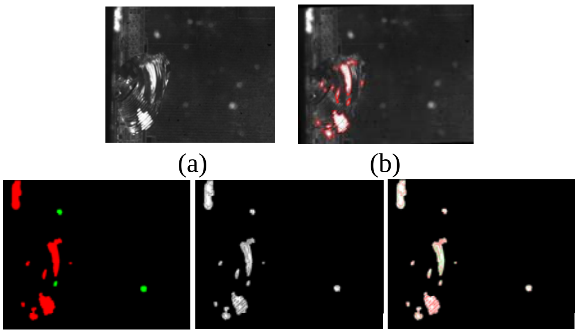

(a) (b)

(c) (d) (e)

Figure 27 The result II of reflection elimination. (a) The final result. (b) The smoothness of candidate defect. (c) The complexity of texture. (d) The structure of defect.

In the second experiment, we use all 137 inspected images to verify proposed low intensity defect detection method. The result is shown in Figure 28. From the result, we can notice that the boundary of chip is correct detected, thus we can detect the low intensity defect certainly.

In the third experiment, we will give time complexity and performance to prove the proposed inspection method is work. For the experiment, 14 inspected images are also used as training data. First, we estimate the execution time for both training phase and test phase. The execution time for training phase is shown in Table 1.

Table 1 The execution time of training phase.

	Training phase
Execution Time (second)	0.002

Table 2 The execution time of the proposed method.

	High intensity defect detection	High+low intensity defect detection
Average Execution Time (second)	0.080	0.115

And the execution time for test phase can be divided into high intensity defect detection and high intensity defect detection plus low intensity defect detection. Because there are two situations for the defect is detected. The first is the high intensity defect detection method detects the defect. And the other is the high intensity defect detection method doesn’t detect, and the low intensity defect detection method does. The execution time for test phase is shown in Table 2. Next we use 53 high intensity defect images as test image, and then observe whether the proposed method can detect high intensity defect or not. Like high intensity defect detection method, low intensity detection method is performed with 16 low intensity defect images as test image. The result is show in Table 3.

Table 3 The result of proposed high intensity defect detection method

Classify as	**High intensity defect** (%)	**Low intensity defect** (%)
Defect	85.0(45)	62.5(10)
Non-defect	15.0(8)	37.5(6)

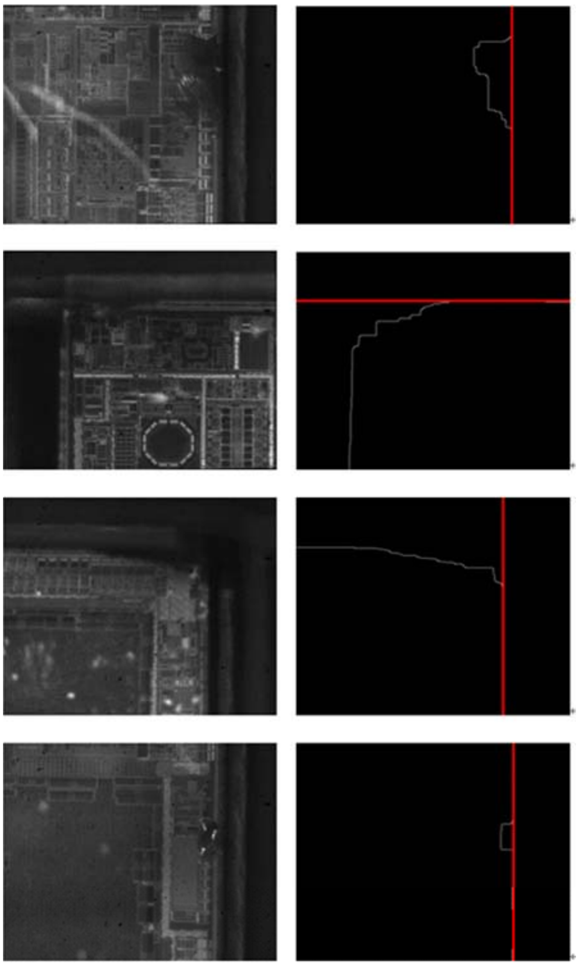

(a) (b)

Figure 28 The results of low intensity defect detection. (a) The input images. (b) The result of proposed method.

For further prove proposed method, we use some statistics to show the relationship between the real answer and classified answer. Four statistics, true positive (TP), false positive (FP), false positive (FP), false negative (FN), are used to indicate the relationship between the real answer and classified answer. Then, we used the commonly prediction performance measures, accuracy, recall [11], and false alarm, as our performance index. The definition of accuracy is the ratio of number of correct detected image and number of test image. The accuracy can be compute by

$$\text{Accuracy} = \frac{TP + TN}{TP + TN + FP + FN} \tag{17}$$

Then the recall measurement is use to estimate the accuracy of detect defect in defect image. Recall is defined as follow

$$\text{Recall} = \frac{TP}{TP + FN} \tag{18}$$

Finally false alarm is the index for error detection. The formulation is defined as

$$\text{False Alarm} = 1 - \frac{TN}{TN + FP} \tag{19}$$

We use 14 inspected images for training data and use these 14 inspected images for testing. And then using remaining 123 inspected images which don not include the training data for testing. The result is shown in Table 4. Our proposed inspection method can achieve 86% for accuracy and 83% for recall and only 11.1% for false alarm. That is to say the proposed method performs good detection result for chip inspection.

Table 4 The performance of proposed method

	Training data	Testing data
Accuracy(%)	92.8	86.0
Recall(%)	100	83.0
False Alarm(%)	20.0	11.1

But under some situation, our method will fail. There two situations for false detection. The first is that there is no defect in the inspected images, but the proposed method still detects the defect. The other one is that there is defect in the inspected images, but the proposed method can't detect the defect. Figure 29 and Figure 30 are examples for the situation that there is no defect in the inspected images, but the proposed method still detect the defect. Figure 29 show that if the detail of chip is similar with defect, proposed high intensity method will fail. In Figure 30, if the boundary of chip is not clear enough, then our method will fail. Figure 31 is an example for the situation that there is defect in the inspected images, but the proposed method can't detect the defect. In Figure 31, if the defect is too small or is similar with the detail of chip, our method fails. To overcome above problems is interesting future works for us.

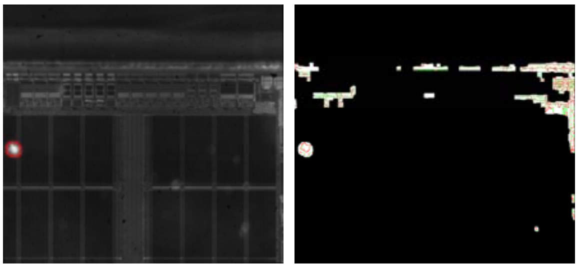

(a) (b)

Figure 29 The failed result of defect detection. (a) The detection result. (b) The structure of texture in candidate defect.

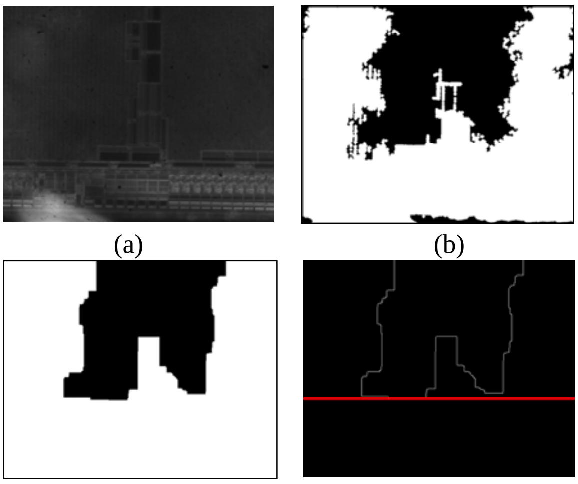

(a) (b) (c) (d)

Figure 30 The failed result of defect detection. (a) The input image. (b) Corresponding energy map. (c) After morphological operation. (d) Final result.

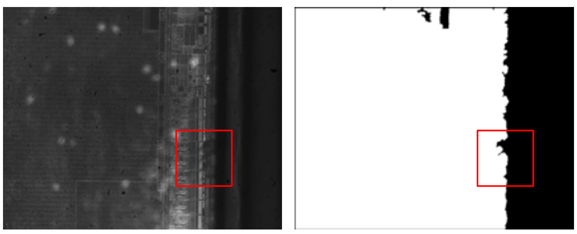

(a) (b)

Figure 31 An example of failed result of defect detection. (a) Input image. (b) Corresponding energy map.

5. Conclusions

In this paper, we proposed a hybrid defect detection algorithm for wafer level chip scale package images. Conventional chip inspection is inefficient. Automatic inspection provides an streamlined alternative method for defect detection. Owing to complex defects, the defects are divided into two kind of defect, high intensity defect and low intensity defect. First of all, for precisely detecting defects, Hough transform is applied to correct the rotation of test image. And then for high intensity defect, a simple threshold method is used to separate the high intensity region as candidate defects. Then the morphology operations are applied to remove noise region and fill up the contour of remaining candidate defects. For each candidate defect, smoothness, complexity of texture and structure of defect are used as features for support vector machine. We find that the low intensity defects always appear at the boundary of chip. Thus boundary defect detection is proposed to solve this problem. First dividing test image into chip region and background. Morphology operations are applied to fill up the chip region. Finally, Hough transform is used to find the boundary of chip. Then compute the distance between contour of chip detected boundary line.

Experimental results show that our proposed method can efficiently detect defects with different size and shape. Owing to proposed learning method and proposed boundary defect detection method, most of defect on the chip can be efficient detected. Our future work is to develop a method for small defect detection.

Acknowledgments

The authors would like to thanks Prof. C. C. Jeng of Dept. of Physics, National Chung Hsing University for providing the test images used in this paper.

References

[1] N. G. Shankar and Z. W. Zhong, "Defect detection on semiconductor wafer surfaces," Microelectronic Engineering, vol. 77, no. 3-4, pp. 337-346, Apr. 2005.

[2] G. Qu, S. L. Wood and C. Teh, "Wafer defect detection using directional morphological gradient techniques," EURASIP Journal on Applied Signal Processing, vol.2002, no.1, pp.686-703, Jan. 2002.

[3] N. G. Shankar and Z. W. Zhong, "Improved segmentation of semiconductor defects using area sieves," Machine Vision and Applications, vol.17, no.1, pp.1-7, Sep. 2005.

[4] C. Y. Chang, C. H. Li, Y. C. Chang and M. D. Jeng, "Wafer defect inspection by neural analysis of region features," Journal of Intelligent Manufacturing, vol.22, no.6, pp. 953-964, Dec. 2009.
[5] C. S. Chen, C. L. Huang and C. W. Yeh, "A hybrid defect detection for in-tray semiconductor chip," The International Journal of Advanced Manufacturing Technology, vol. 65, no.1-4, pp. 43-56, Mar. 2013.
[6] IH. Witten and E. Frank, *Data Mining: Practical machine learning tools and techniques*, Morgan Kaufmann, 2005.
[7] J. Canny, "A computational approach to edge detection," IEEE Transactions on Pattern Analysis and Machine Intelligence, vol. 8, No.6, Nov. 1986.
[8] R. O. Duda and P. E. Hart, "Use of the Hough transformation to detect lines and curves in pictures," Communications of the ACM, vol.15, no.1, pp.11-15, Jan.1972.
[9] A. W. Paeth, "A fast algorithm for general raster rotation," Graphics Interface. vol. 86, pp.77-81, 1986.
[10] R. C. Gonzalez and R. E. Woods, *Digital Image Processing* 2nd ed., Prentice Hall, 2002.
[11] C. Cortes and V. Vapnik, "Support-vector networks," Machine learning, vol. 20, no.3, pp. 273-297, Sep 1995.